Propagating wavelet simulation

Linping Dong and Gary F. Margrave

ABSTRACT

In investigating the variation of nonstationary wavelets in a medium with attenuation, we apply the 45-degree wave equation to wavefield upward continuation with a constant-Q model. The amplitude variation and phase property of the propagating wavelet are simulated and then validated by the spectral ratio and spiking deconvolution approach. The synthetic data are also compared to the forward-Q-filtered trace which is generated by another method. The estimated Q value from synthetic data by the spectral ratio method is quite close to the Q value given in the model. The result of spiking deconvolution shows the wavelet in the synthetic data is effectively minimum phase. A layered-Q model is also tested. The average Q estimated by spectral ratio method is reliable for the noise free data.

INTRODUCTION

The attenuation of seismic energy by the earth and the resulting nonstationary recorded data traces are fundamental issues in seismic data processing and interpretation. There are two separate approaches to seismic pulse propagation and dispersion in attenuating media. The first assumes Q depends on frequency (Ricker, 1953, Kolsky, 1955, Aki and Richards, 1980). The second approach assumes Q is independent of frequency, that is the constant-Q model. Q is then used to calculate pulse broadening and dispersion (Futterman, 1962; Carpenter, 1966; Kjartansson, 1979). Futterman derived a theoretical dispersion relation for materials with a constant-Q. Wuenschel (1965) experimentally showed Plexiglas and shale to exhibit a similar dispersion relation. Earth materials have been shown to have a nearly constant-Q over the seismic frequency range (Spencer, 1981). So the constant-Q model has gained greater acceptability in seismology.

The relationship between the attenuation and dispersion provides an important way to include the effects of attenuation into seismic synthetic data. The basic dispersion relation used in generation of seismograms and inverse-Q filtering is derived by Kjartansson (1979). He developed practical techniques for incorporating the effect of attenuation on wave propagation in a medium where Q varies with depth but not with frequency. He also provided a convolution operator by which the effect of attenuation can be easily included in synthetic seismograms. The dispersion relation given by Futterman can be derived from Kjartansson's equation and may be used in wave propagation too. A good example using Futterman's equation in inverse-Q filtering is provided by Hargreaves and Calvert (1991). They consider the process of inverse-Q filtering as a migration with the phase-shift method.

There are many methods for determining the Q value. Among these, the spectral ratio approach is more accurate than others if the data is noise free (Tonn, 1991).

Synthetic data is a good candidate for this method. So all the estimated Q values in this project are calculated using spectral ratio approach.

The purpose of this paper is to describe the behaviour of a constant-Q model by acoustic-wave equation modelling in the frequency-space domain, based on an understanding of the relationship between attenuation and dispersion. The frequency-space domain wavefield continuation was chosen in favour of other methods because the dispersion relation can be easily included in the wave equation and Q value can vary in both vertical and horizontal directions.

ATTENUATION, DISPERSION, AND CONSTANT-Q MODEL

Here we provide a review of the fundamental concepts associated with this research. Seismic attenuation can be caused by many factors such as absorption, geometric spreading, transmission, mode-conversion, and intrabed multiples and scattering (Schoepp, 1998). Anelastic attenuation is the process by which rocks convert compressional and shear waves into heat. This process causes a loss of high-frequency energy with increasing arrival time and also a time-varying distortion of wavelet phase. This process can be measured by a dimensionless value, Q, given by equation (Aki and Richards, 1980)

$$\frac{1}{Q(\omega)} = -\frac{\Delta E}{2\pi E}, \tag{1}$$

where E is the peak (or average) strain energy stored in a volume of material; $-\Delta E$ is the energy lost in each cycle because of imperfections in the elasticity of the material; and $Q(\omega)$ is a quality factor which characterizes this energy loss within a cycle.

Constant Q means the Q value is independent of frequency but can vary in the space and time. Under the assumptions of linearity and causality, the effect of the constant-Q attenuation can be represented with the equation (Appendix A) given by Margrave (1998)

$$\alpha_Q(t,f) = e^{-\pi\frac{ft}{Q} + iH\left(\frac{\pi ft}{Q}\right)}, \tag{2}$$

where H represents the Hilbert transform, f is the frequency and t, the traveltime. Space $\alpha_Q(t,f)$ is an impulse response in the time-frequency domain. It is equivalent to a forward-Q filter, including both attenuation and dispersion effects.

Dispersion, the variation of seismic velocity versus frequency, is a consequence of the requirement that wave propagation in an absorbing medium must be causal (Aki and Richards, 1980). A constant-Q attenuation medium disperses propagating mechanical waves. Otherwise, the wave propagation will violate elementary notions of causality. So, this requirement also implies that the phase spectrum of the attenuated response to an impulse is the Hilbert transform of log of its amplitude

spectrum (Aki and Richards, 1980). If the phase spectrum of a pulse can be computed by the Hilbert transform of the log of its amplitude spectrum, we call the pulse a minimum-phase wavelet (Margrave, 2001). Equation (2) is also a minimum-phase filter. When a minimum-phase source signature experiences an attenuation, this process is equivalent to convolving the signature with a attenuated response to an impulse. The output of the convolution maintains the minimum-phase characteristic.

CONTINUATION USING A FINITE-DIFFERENCE SOLUTION

In a 2D medium, the wave equation for compressional waves in space-frequency domain can be written as

$$\frac{\partial^2 P}{\partial z^2} = -\frac{\partial^2 P}{\partial x^2} - \frac{\omega^2}{v^2} P , \tag{3}$$

where $P = P(x,z,\omega)$ represents the pressure wavefield; $v = v(x,z)$ is the velocity, and ω is angular frequency. Equation (3) is a two-way wave equation. If we directly use it in wavefield continuation, multiples will be generated when the velocity is not a continuous function of space. So, a one-way equation is useful if multiples are not wanted. The square root equation can be directly derived from equation (3); that is

$$\frac{\partial P}{\partial z} = \pm \frac{i\omega}{v} \sqrt{1 + \frac{v^2}{\omega^2} \frac{\partial^2}{\partial x^2}} P , \tag{4}$$

where the plus sign on the right side of the equation represents the upcoming wave and the minus sign the downgoing wave, while the minus sign convention in forward Fourier transform is chosen. Based on the exploding reflector concept, the zero-offset reflected wave recorded at the surface can be simulated by upward continuation of the exploding reflector using a half velocity from certain depth. So we chose the minus sign in equation (4).

To approximate equation (4) with a finite-difference equation, it needs to be approximated first by the continued fraction method (Lee and Suh, 1985):

$$Y_{n+1} = \frac{S}{2 + Y_n} , \tag{5}$$

where

$$S = \frac{v^2}{\omega^2} \frac{\partial^2}{x^2} , \tag{6}$$

$$Y = (1 + S)^{\frac{1}{2}} - 1 , \tag{7}$$

and Y_n is the nth order approximation of Y. Y_0 is zero. The 2nd order approximation of equation (4) for the downgoing wavefield then can be written as a conventional 45-degree equation (Lee and Suh, 1985):

$$\frac{\partial P}{\partial z} = -\frac{i\omega}{v}(1 + Y_2)P \; , \tag{8}$$

where

$$Y_2 = \frac{S}{2 + Y_1} = \frac{S}{2 + \dfrac{S}{2 + Y_0}} \; . \tag{9}$$

Substituting equation (6) and (9) into equation (8), then equation (8) can be expressed as:

$$\frac{\partial P}{\partial z} = -\frac{i\omega}{v}P - \frac{i\omega}{v}\frac{\dfrac{v^2}{\omega^2}\dfrac{\partial^2}{\partial x^2}}{2 + \dfrac{v^2}{2\omega^2}\dfrac{\partial^2}{\partial x^2}}P \; , \tag{10}$$

The wavefield P is related to time-shifted wavefield P' (Yilmaz, 1987):

$$P = p'e^{-i\omega\frac{z}{\bar{v}}} \; , \tag{11}$$

where $\dfrac{z}{\bar{v}}$ is the retarded time at depth z. The derivative of P over z is

$$\frac{\partial P}{\partial z} = \left(\frac{\partial}{\partial z} - i\frac{\omega}{\bar{v}}\right)P'e^{-i\omega\frac{z}{\bar{v}}} \tag{12}$$

Substituting equation (11) and (12) into equation (10) means it can be written as:

$$\frac{\partial P'}{\partial z} = (\frac{i\omega}{\bar{v}} - \frac{i\omega}{v})P' - \frac{i\omega}{v}\frac{\dfrac{v^2}{\omega^2}\dfrac{\partial^2}{\partial x^2}}{2 + \dfrac{v^2}{2\omega^2}\dfrac{\partial^2}{\partial x^2}}P' \tag{13}$$

If the horizontal velocity variation can be ignored, $\bar{v} \approx v$, equation (13) can be expressed as

$$\frac{4\omega^2}{v^2}\frac{\partial P'}{\partial z} + \frac{\partial^3 P'}{\partial x^2 \partial z} + \frac{2i\omega}{v}\frac{\partial^2 P'}{\partial x^2} = 0 \tag{14}$$

After getting the solution $P'(x, z, \omega)$ from equation (14), then we use equation (11) to shift the wavefield from depth z to surface and finish the wavefield extrapolation at depth z. The synthetic data is $P(x, z = 0, t)$, which is the inverse Fourier transform of the final solution from equation (11).

Now we need to include the effect of the constant-Q attenuation in equations (11) and (14). The constant-Q theory of Kjartansson and others is the simplest attenuation theory. It can be easily incorporated in the wavefield continuation. The relationship between the dispersion and constant-Q attenuation given by Kjartansson (1979) is

$$\frac{v(\omega)}{v(\omega_0)} = \left(\frac{i\omega}{\omega_0}\right)^{\gamma} \, , \tag{15}$$

where

$$\gamma = \frac{1}{\pi}\tan^{-1}\left(\frac{1}{Q}\right) \, , \tag{16}$$

Q is the quality factor, $v(\omega)$ is the complex phase velocity, $v(\omega_0)$ is the phase velocity at reference frequency ω_0. Here we replace the real velocity, v, in equation (11) and (14) for $v(\omega)$. That is:

$$\bar{v} \approx v \Leftrightarrow v(\omega) = v(\omega_0)\left(\frac{i\omega}{\omega_0}\right)^{\gamma} = v\left(\frac{\omega}{\omega_0}\right)^{\gamma}\exp\left(\frac{\pi}{2}i\gamma\right), \tag{17}$$

where $v(\omega_0)$ is chosen to be the real velocity given in the model. Then we change the elastic wave equation to the anelastic wave equation and incorporate the attenuation effect on the wavefield continuation scheme (Aki and Richards, 1980).

Using the Crank-Nicolson difference method and replacing v for $v(\omega)$, the solution for equation (14) can be represented with the finite-difference equation (appendix A):

$$aP'_{m-1,n+1} + bP'_{m,n+1} + aP'_{m+1,n+1} = cP'_{m-1,n} + dP'_{m,n} + cP'_{m+1,n}, \tag{18}$$

with the notations of:

$$P'_{m,n} = P'(m\delta x, n\delta z),$$

$$a = \frac{1}{\delta z}\left(\frac{2iv(\omega)}{\omega} + \frac{2i\omega\delta x^2}{v(\omega)\delta z}\beta\right) - 0.5 \qquad\qquad b = -2a + \frac{2i\omega\delta x^2}{v(\omega)\delta z}$$

$$c = a + 1 \; ; \qquad\qquad\qquad\qquad\qquad d = -2c - \frac{2i\omega\delta x^2}{v(\omega)\delta z},$$

where β is the factor in second order derivative:

$$\frac{\partial^2 P^{'}}{\partial x^2} = \frac{1}{(\delta x)^2} \frac{T}{1 + \beta T} P^{'}. \tag{19}$$

The computing process includes several steps:

1. Given a model in (x, z) domain as well as a source signature, $P^{'}(x, z, t = 0)$.

2. From maximum depth level, for each depth step, solve the equation (16) to get the monochromatic wavefield at a given depth and then shift the wavefield upward to surface.

3. At depth $z = 0$, transfer the wavefield $P(x, z = 0, \omega)$ to time domain.

4. Finally get the synthetic data $P(x, z = 0, t)$ by inverse Fourier transform.

ANALYSIS OF UPWARD CONTINUATION

Figure 1(a) is the model used to generate the synthetic data. There are three scatter points in the model. Velocity is equal to 1000 m/sec and Q is a constant. Figure 1(b) displays a minimum-phase source signature and its amplitude spectrum. The dominant frequency in the spectrum is 80 Hz. This signature is used for all the tests in the paper. The synthetic time sections created from the model given in Figure 1 are displayed from Figure 2 corresponding to three Q values, 50, 100, and 200 respectively. There are three diffractions on the zero-offset sections. We chose only 25 traces and 256 samples for each trace in the synthetic data so as to speed up the calculation.

The synthetic data then are validated to verify the method used in simulating the constant-Q attenuation procedure. There are three methods being applied to check the phase property, amplitude and waveform of the propagating pulse.

At first, the phase property of the propagating wavelet is tested. We have discussed that, when a minimum-phase source signature travels through a medium with constant-Q attenuation, the output is still minimum-phase. Spiking deconvolution can be used to test the phase characteristics of the synthetic data. According to the minimum-phase assumption in spiking deconvolution, if a wavelet is minimum-phase it will be compressed into an impulse after deconvolution. Otherwise, it cannot be an impulse. So spiking deconvolution can validate whether the propagating wavelet is minimum-phase or not. Figure 3 shows a synthetic trace generated with a minimum-phase source signature and the result of spiking deconvolution. The Q value is 50. As shown in the trace after deconvolution, the pulse is approximately an impulse. Figure 4 displays the similar result with Q equal to 100. The results shown in both figures are consistent with the theory we discussed before. Then we can say the reflected pulse is minimum-phase. Figure 5 shows a propagating wavelet reflected from three subsurface and then deconvolution with a stationary wavelet. It is interesting that

although they all become the spike but with different width. Comparing Figures 3 and 4, we can infer that for the seismic data from an attenuating medium, nonstationary deconvolution should be used to improve the resolution in both shallow and deep areas.

An important verification for the approach used to simulate waves in a constant-Q attenuation media is that the estimated Q from a reflected pulse at some time should approximate the given Q at the corresponding reflector in the model.

The spectral ratio method is the most commonly used method of Q estimation. In this method, Q is estimated from the log ratio of the amplitude spectra of a wave at two different times (White, 1992). The amplitude spectrum of a pulse experiencing a constant-Q attenuation can be given by (Aki and Richards, 1980):

$$| A(t,f) |=| A_0(f) | e^{-\pi f t/Q} \; , \tag{20}$$

where t is the traveltime of the pulse, $\left| A_0(f) \right|$ is the amplitude spectrum of the source signature of the pulse and $| A(t,f) |$ is the attenuated amplitude spectrum of the pulse. Equation (20) at some time, t_2, is divided by the same equation at an early time, t_1:

$$\frac{| A(t_2,f) |}{| A(t_1,f) |} = e^{-\pi f (t_2-t_1)/Q} \; . \tag{21}$$

After taking the natural logarithm, equation (22) is converted into

$$\ln\left[\frac{| A(t_2,f) |}{| A(t_1,f) |}\right] = -\pi f (t_2 - t_1)/Q \; . \tag{22}$$

In equation (22), Q is calculated from the slope of the least-square regression against frequency of the log spectral ratio. This equation is accurate for noise-free data (Tonn, 1991). Figure 6 shows a group of traces which are generated with different Q attenuation on the same model. Figure 7 shows the amplitude spectra of reflection waves from third subsurface, corresponding to each trace in Figure 6. With Q decreasing, the high-frequency components are attenuated gradually and the dominant frequency shifts toward lower frequency. Figure 8 is the log of the amplitude spectrum ratio of the shallow and deep pulse in Figure 6. For each Q, the log curve is a straight line. For a given time difference, $t_2 - t_1$, if the term on the left of the equation (22) is linearly proportional to frequency, the Q is independent of frequency. Figure 9 shows the estimated Q on the Figure 8 with spectral ratio method. The given Q and estimated values are also listed in Table 1. Because the

error in the arrival time and frequency can be negligible in this case, so the error in estimating Q can be attributed to the error in calculating amplitude spectrum ratio, and to the notches in the spectra caused by the ghost or multiple. If the two pulses used in estimating Q are too close, the accuracy of calculation of both their amplitude spectra and Q will decrease.

Table 1. Given Q in the model and estimated Q by spectral ratio methods.

given Q value	10	20	30	40	50	60	70	80	90	100
estimated Q	10.6	20.52	30.63	40.74	50.92	60.9	71.3	81.6	91.5	102.1

The calculated Q value is reliable if the data is noise-free (Tonn, 1991). Otherwise, this method can be inaccurate. The amplitude spectra of two noisy synthetic traces with signal-to-noise ratio equal to 5 and their log ratio are displayed in Figures 10 and 11. The Q value given in the model is 50. An estimated value greatly departing from the given value means the noise suppression is very important for spectral ratio method.

Finally, the synthetic trace is compared with a constant-Q filtered trace. The filter used in this comparison is designed by Margrave (1996) using constant-Q theory of Kjartansson (1979). In the constant-Q and dispersive material, the Fourier transform of the impulse response can be represented by (Kjartansson, 1979):

$$B(t,f) = e^{-\frac{\pi |f| t}{Q}} e^{i2\pi ft\left(1 - \frac{1}{\frac{1}{\pi Q}\left|\frac{f}{f_{nyq}}\right|}\right)}, \qquad (23)$$

If we do an inverse Fourier transform on equation (24), we get

$$b(t,\tau) = IFT\big[B(t,f)\big], \qquad (24)$$

where *IFT* is the inverse Fourier transform, f_{nyq} is Nyquist frequency, and t is the arrival time of waves from source to some locations. Equation (23) and (24) are nonstationary forward-Q filters represented in frequency and time domain respectively. The array, $b(t,\tau)$, is also called the Q matrix that is shown in Figure 12 with two different Q values. The comparison process includes several steps: at first, use the same source signature as one in the wavefield continuation to convolve with $b(t_i,\tau)$ where time, t_i, is arrival time calculated at the depth of the corresponding reflector. Then add all the results from convolution at different arrival times to get a Q-filtered trace. Finally display the filtered trace together with synthetic trace. In Figure 13 we compare the attenuated traces from wavefield continuation and Q matrix respectively. The results are very close each other.

The validation shows that the modelling with wavefield continuation in constant-Q attenuation medium is reasonable and useful.

A LAYERED-Q MODEL

The mechanism of attenuation in the real earth is better modelled by layers with different Q values. This variation is caused mainly by rock type, saturation state, pressure and amplitude of the acoustic wave (Toksoz, 1981). It may be possible to deduce these properties by variation in Q value, especially for the existence of the gas or fluid in the earth. So it may be reasonable to consider the effect of the local Q value variation on the average Q of a layered system. Like the concepts describing the velocity, we can call the Q value corresponding to a layer the interval Q value which is a constant within the layer. The summed effect of the different interval Q values is called the average Q value in this project. Suppose there is a layered model (with layers $i = 1, n$) with interval Q equal to Q_i for i^{th} layer and arrival time of wave from i^{th} reflector equal to t_i. From equation (21), the amplitude spectrum of a wave from the bottom boundaries of the first layer can be written as:

$$| A(t_1, f) | = | A_0(f) | e^{-\pi f t_1 / Q_1} . \tag{25}$$

The amplitude spectrum of a wave from the second reflector is

$$| A(t_{2,} f) | = | A_0(f) | e^{-\pi f (t_1 / Q_1 + (t_2 - t_1) / Q_2)} , \tag{26}$$

and the amplitude spectrum of a wave from the nth reflector is

$$| A(t_{n,} f) | = | A_0(f) | e^{-\pi f (t_1 / Q_1 + (t_2 - t_1) / Q_2 + \dots + (t_n - t_{n-1}) / Q_n)} = | A_0(f) | e^{-\pi f \sum_1^n \Delta t_i / Q_i} . \tag{27}$$

Then average Q can be defined as

$$Q_{ave}(n) = \frac{\tau}{\sum_1^n \Delta t_i / Q_i} , \tag{28}$$

where τ is the arrival time of the wave from i^{th} reflector, Δt_i is the time difference between the ith and $(i-1)^{th}$ reflectors, and Q_{ave} is the average Q. Equation (28) shows that Q_{ave} is bounded by minimum and maximum Q_i. When all the layers have a same Q_i, it is equal to Q_{ave}. The layer with the smallest Q_i can obviously decrease Q_{ave} when other two parameters have a gentle variation. This is a useful indicator in the identification of the gas or fluid layer. Limited by seismic resolution, sometimes we cannot delineate the target layer or get Q_i. By comparing Q_{ave} from different

depth, we can get some useful information relating to Q_i. To show the effect of the Q_i on Q_{ave} in the layered system, first we generate a set of synthetic data and then calculate the Q_{ave} using the spectral ratio method. The estimated Q_{ave} and given Q_i are displayed in Figure 14. Q_{ave} from two approaches is also shown in Table 2. In Table 2, Q_1, Q_2, and Q_3 represent the given Q values for three layers. $Q_{ave-est}$ and $Q_{ave-eqn}$ are the average Q values of the 2nd and 3rd layers from the spectral ratio and equation (28) respectively. The curve in Figure 14 is calculated from the data listed on Table 2. We see that the $Q_{ave-est}$ is a good approximation of the $Q_{ave-eqn}$. But they are not exactly same. Figure 14 also shows that the layer with a lower Q value dominates the average Q estimation for a two-layered model. The smaller the interval Q, the more closely the average Q approximates it.

Table 2. Model parameter for average Q analysis

Q_2	Q_3	$Q_{ave-est}$	$Q_{ave-eqn}$	Velocity (m/sec)	Depth (m)
100	10	26	21	V1=1500	D1=24
100	20	41	37	V2=1500	D2=60
100	30	53	50	V3=2000	D3=96
100	40	64	61		
100	50	73	70		
100	60	81	78		
100	70	87	85		
100	80	92	90		
100	90	96	95		
100	100	102	100		

$Q_1 = 50$

From the above discussion we know that the spectral ratio method can be used for determining the average Q in a layered-Q model.

CONCLUSION

Space-frequency domain wavefield continuation can be used in both forward- and inverse-Q filtering. The Q value estimated by spectral ratio method on the synthetic data is close to the given Q. This means the relative amplitude in the synthetic data is correct and energy attenuation of the wavefield based on the constant-Q model is reasonable. The deconvolved trace shows that the pulses in synthetic data are minimum phase, which is the result of the dispersive model. Comparison of the synthetic data and the forward-Q filtered trace shows that the difference between them is mainly caused by time advancement in attenuated synthetic trace and low-pass effect of the wavefield continuation method. This problem needs to be further investigated. The spectral ratio method is also verified. It is accurate for the noise-free data, but it fails for a noise-contaminated trace. It can be used to estimate both

interval and average Q for a layered-Q model. In a layered-Q system, a layer with very low interval Q can obviously affect average Q.

ACKNOWLEDGEMENTS

We would like to thank the sponsors for their support of the CREWES project.

REFERENCES

Aki, K. and Richards, P.G., 1980, Quantitative Seismology: Theory and Methods, Vol. 2, W. H. Freeman and Company.

Bancroft, J.C., 2001, A Practical Understanding of Pre- and Poststack Migrations, Society of Exploration Geophysicists.

Carpenter, E.W., Absorption of Elastic Wave, Seismic Wave Attenuation, Geophysical Reprint Series, No. 2.

Futterman, W.I., 1962, Dispersive body wave: Journal of Geophysical Research, **67**, 5279-5291.

Kjartansson, E., 1979, Constant Q-wave propagation and attenuation: Journal of Geophysical Research, **84**, 4737-4748.

Kolsky, H., 1955, The propagation of stress pulses in viscoelastic solids: Philosophical Magazine, **1**, 693-710.

Hargreave, N.D. and Calvert, A.J., 1991, Inverse-Q filtering by Fourier transform: Geophysics, **56**, 519-527.

Lee, M.W. and Suh, S.Y., 1985, Optimization of one-way wave equations: Geophysics, **50**, 1634-1637.

Margrave, G.F., 1996, qmatrix.m: matlab code, CREWES

Margrave, G.F., 1998, Theory of nonstationary linear filtering in the Fourier domain with application to time-variant filtering: Geophysics, **63**, 244-259.

Margrave, G.F., 2001, Methods of seismic data processing, Geophysics 657 Course Lecture Notes: University of Calgary.

Ricker, N., 1953, The form and laws of propagation of seismic wavelets, Geophysics, **18**, 10-40

Schoepp, A.R. 1998, Improving Seismic Resolution with Nonstationary Deconvolution, M.Sc. Thesis: University of Calgary

Spencer, J.W. Jr., 1981, Stress relaxations at low frequencies in fluid-saturated rocks: attenuation and modulus dispersion: J. Geophys. Res., **86**, 1803-1812.

Toksoz, M.N. and Johnston, D.H., 1981, Seismic Wave Attenuation, Geophysics Reprint Series No. 2, Society of Exploration Geophysicists.

Tonn, R., 1991, The determination of the seismic quality factor Q from VSP data: a comparison of different computational methods: Geophysical Prospecting, **39**, 1-27.

White, R.E., 1992, The accuracy of estimating Q from seismic data: Geophysics, **57**, 1508-1511.

Wuenschel, P.C., 1965, Dispersive body waves-an experimental study: Geophysics, **30**, 539-551.

Yilmaz, O., 1987, Seismic Data Processing (Text), SEG.

APPENDIX A

Equation (2) can be derived as follows:

A stationary source signature should be a causal wavelet. That is

$$u\ (x=0,t)=0, \text{ for } t<0 \tag{A-1}$$

At $x>0$, each Fourier component of u can be factored as:

$$u(x,\omega) = u(0,\omega)e^{ikx} , \qquad \text{(A-2)}$$

where $k = \dfrac{\omega}{v}$ is the wavenumber and ω is the angular frequency. Attenuation can be introduced into this model by allowing either k or ω to be complex. Dispersion can also be added in the model by allowing velocity to depend on frequency. Let k be complex and velocity be a function of the frequency result in

$$u(x,\omega) = u(0,\omega)e^{i(\frac{w}{v(\omega)} + i\alpha(\omega))x} , \qquad \text{(A-3)}$$

where

$$\alpha(\omega) = \frac{\omega}{2v(\omega)Q} , \qquad \text{(A-4)}$$

and $\alpha(\omega)$ is the attenuation coefficient. With the assumption of the linear superposition, the wave at (x,t) is

$$u(x,t) = \frac{1}{2\pi}\int_{-\infty}^{\infty} u(0,\omega)e^{i(kx-\omega t)}d\omega , \qquad \text{(A-5)}$$

which is equivalent to the convolution of $u(0,t)$ with

$$p(x,t) = \frac{1}{2\pi}\int_{-\infty}^{\infty} e^{i(kx-wt)}d\omega , \qquad \text{(A-6)}$$

where $p(x,t)$ is the attenuated response to an impulse. Requiring this response to be causal, that is

$$p(x,t) = 0 , \text{ for } t < 0, \qquad \text{(A-7)}$$

implies (Aki and Richards, 1980):

$$\frac{\omega}{v(\omega)} = H(\alpha(\omega)), \qquad \text{(A-8)}$$

where $H(\alpha(\omega))$ is the Hilbert transform of the attenuation coefficient. Then we introduce the constant-Q attenuation coefficient (A-4) and get an attenuated response in the frequency domain

$$e^{(-\frac{\omega}{2v(\omega)Q}+iH(\frac{\omega}{2v(\omega)Q}))x} = e^{-\frac{\pi f t}{Q}+iH(\frac{\pi f t}{Q})} , \tag{A-9}$$

where $v(\omega)$ is the complex phase velocity.

APPENDIX B

For the equation (14),

$$\frac{4\omega^2}{v^2}\frac{\partial P^{'}}{\partial z} + \frac{\partial^3 P^{'}}{\partial x^2 \partial z} + \frac{2i\omega}{v}\frac{\partial^2 P^{'}}{\partial x^2} = 0 , \tag{B-1}$$

let

$$\frac{\partial P^{'}}{\partial z} = \frac{1}{\delta z}\left(P^{'}_{n+1} - P^{'}_{n}\right), \tag{B-2}$$

$$\frac{\partial^2 P^{'}}{\partial x^2} = \frac{1}{\delta x^2}\frac{T}{1+\beta T}(\theta P^{'}_{n+1} + (1-\theta)P^{'}_{n}), \tag{B-3}$$

and $T = (1,-2,1)$. Substitute (B-2) and (B-3) into (B-1) and replace v for $v(\omega)$, then (B-1) can be written as

$$\frac{4\omega^2}{v^2(\omega)}\frac{1}{\delta z}\left(P^{'}_{n+1} - P^{'}_{n}\right) + \frac{1}{\delta z \delta x^2}\frac{T}{1+\beta T}\left(P^{'}_{n+1} - P^{'}_{n}\right) + \frac{2i\omega}{v(\omega)}\frac{T}{1+\beta T}\left(\theta P^{'}_{n+1} + (1-\theta)P^{'}_{n}\right) = 0 \tag{B-4}$$

Note that when substituting (B-3) for the second term on the left side of equation (B-1), the θ equals to zero and for the third term θ is 0.5. Now we divide equation (B-4) by $1+\beta T$ and use operator T. Then we get a finite-difference approximation for equation (B-1)

$$aP^{'}_{m-1,n+1} + bP^{'}_{m,n+1} + aP^{'}_{m+1,n+1} = cP^{'}_{m-1,n} + dP^{'}_{m,n} + cP^{'}_{m+1,n} , \tag{B-5}$$

with the notations of:

$$P'_{m,n} = P'(m\delta x, n\delta z)$$

$$a = \frac{1}{\delta z}\left(\frac{2iv(\omega)}{\omega} + \frac{2i\omega\delta x^2}{v(\omega)\delta z}\beta\right) - 0.5;$$

$$b = -2a + \frac{2i\omega\delta x^2}{v(\omega)\delta z}$$

$$c = a + 1;$$

$$d = -2c - \frac{2i\omega\delta x^2}{v(\omega)\delta z}$$
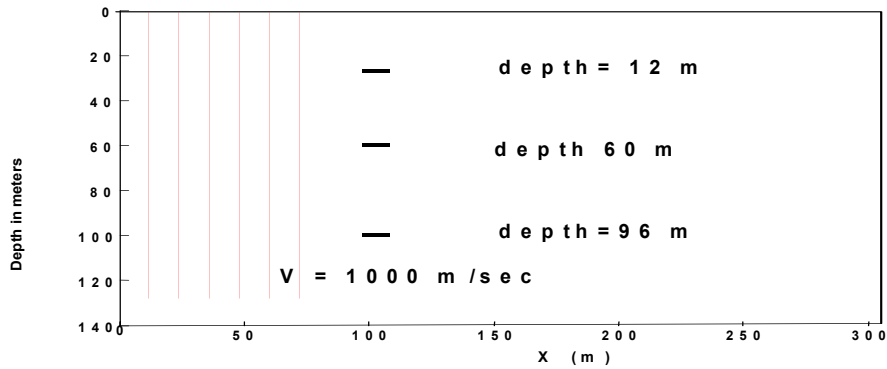
FIG. 1(a): A constant-Q model with three scatterpoints
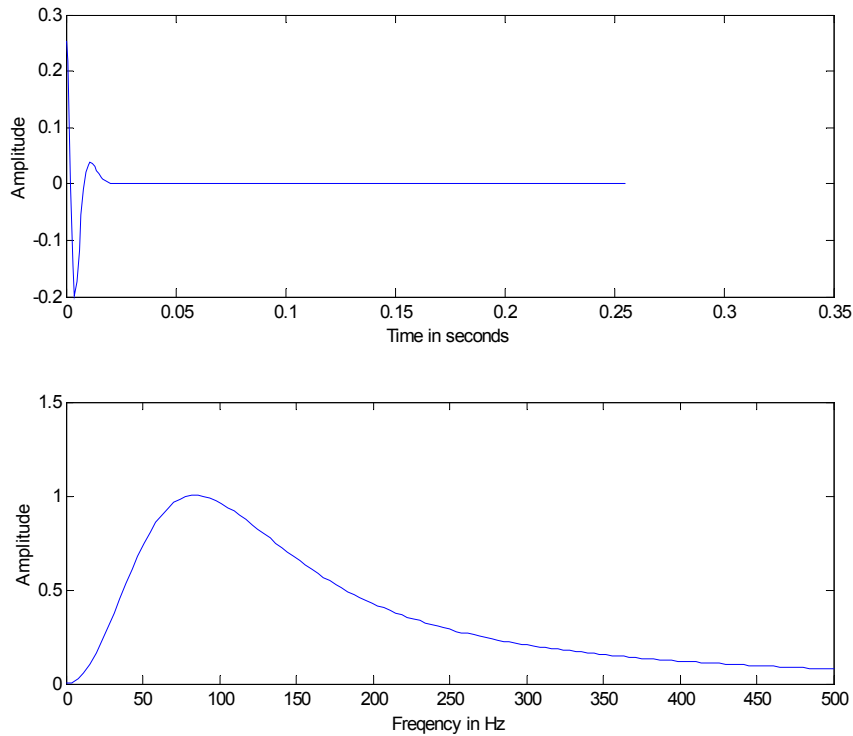
FIG. 1(b): The source signature and its amplitude spectrum
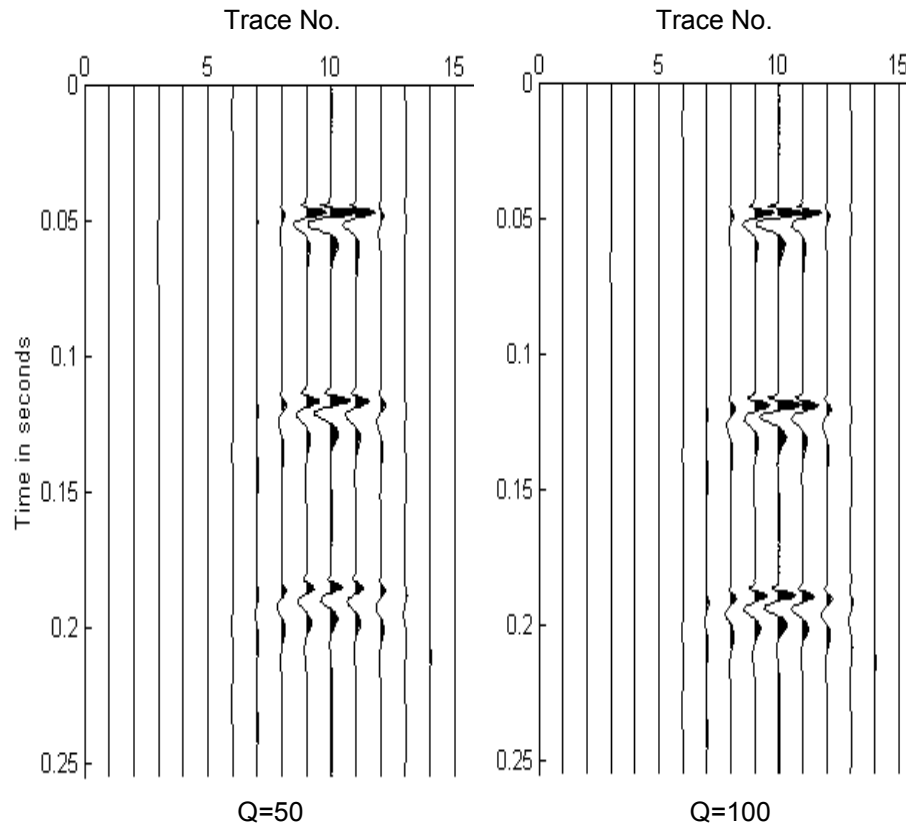
FIG. 2: Synthetic diffraction with different Q values.
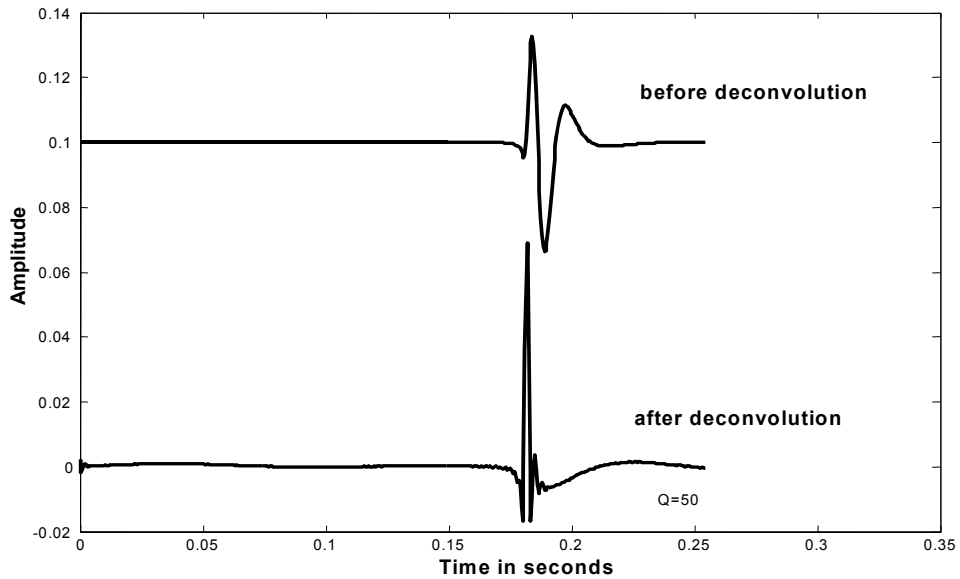
FIG. 3: Synthetic signal with Q equal to 50 and the deconvolved result.
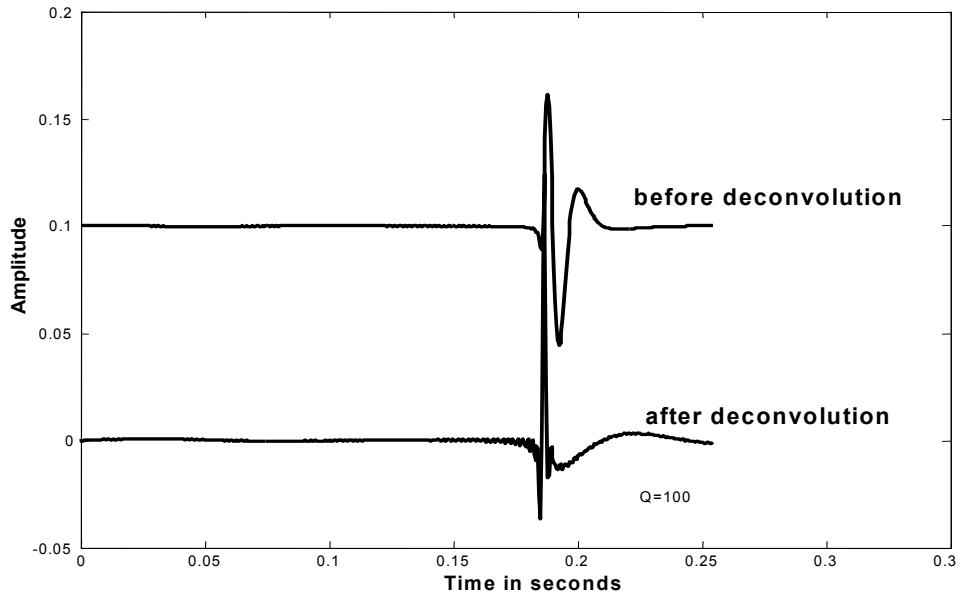
FIG. 4: Synthetic signal with Q equal to 100 and the deconvolved result.
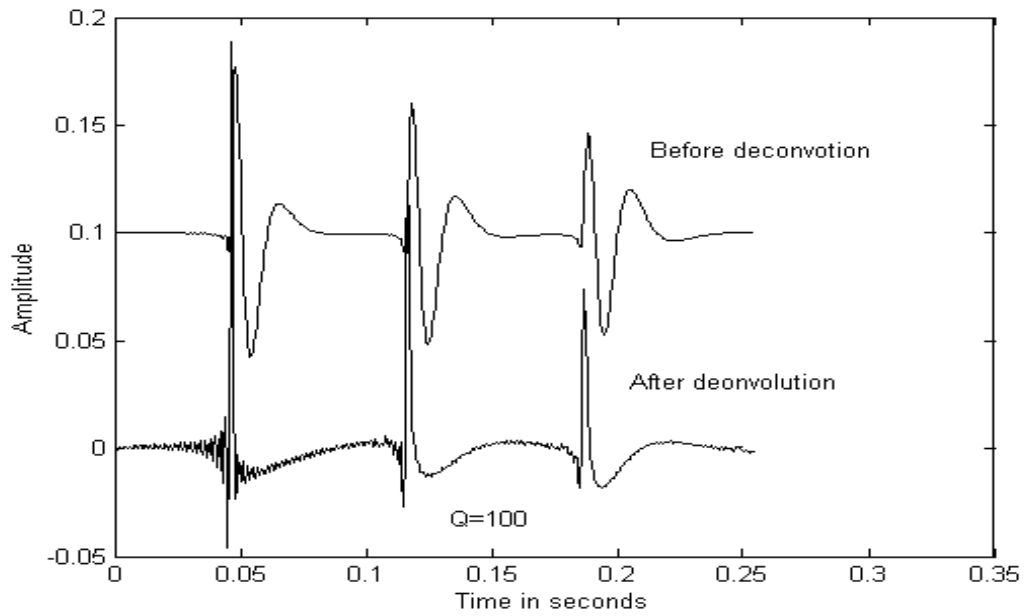
FIG. 5: Synthetic trace and deconvolved trace with Q =100.
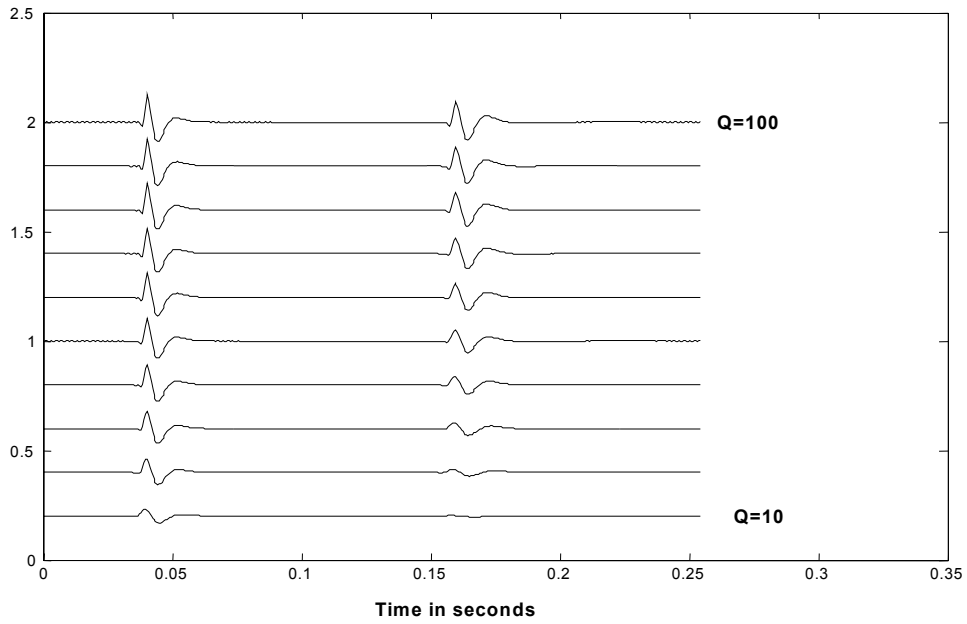
FIG. 6. Traces with different Q attenuation.
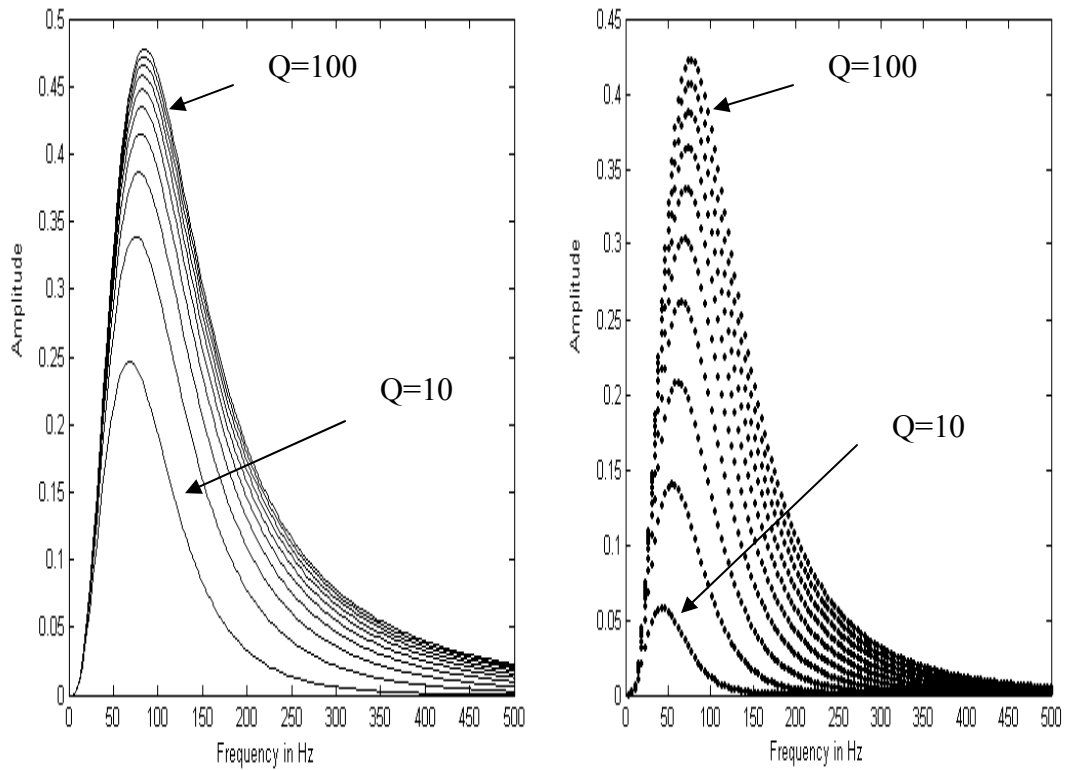
FIG. 7: Amplitude spectra corresponding to the first (left) and the third (right) pulse for each trace in Figure 6.
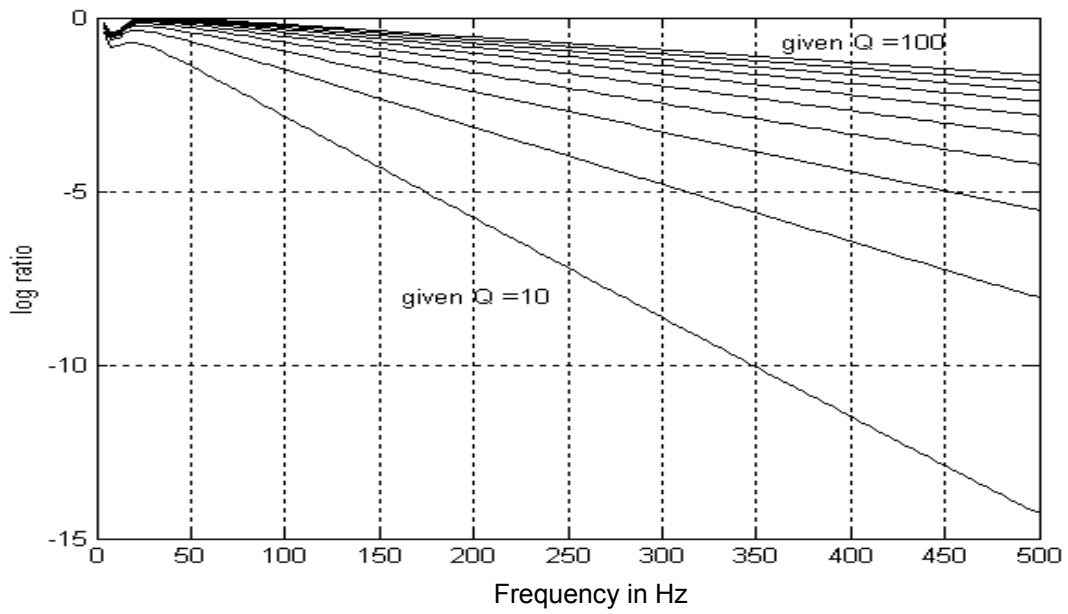
FIG. 8: Log ratios of the amplitude spectra.
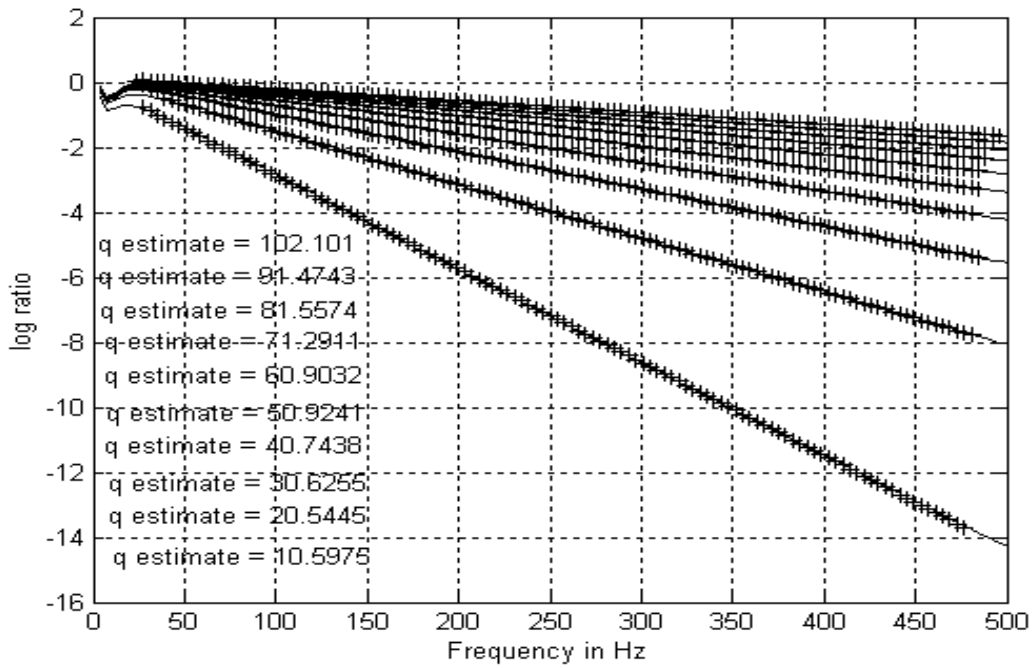
FIG. 9: Estimated Q values by the spectral ratio method.
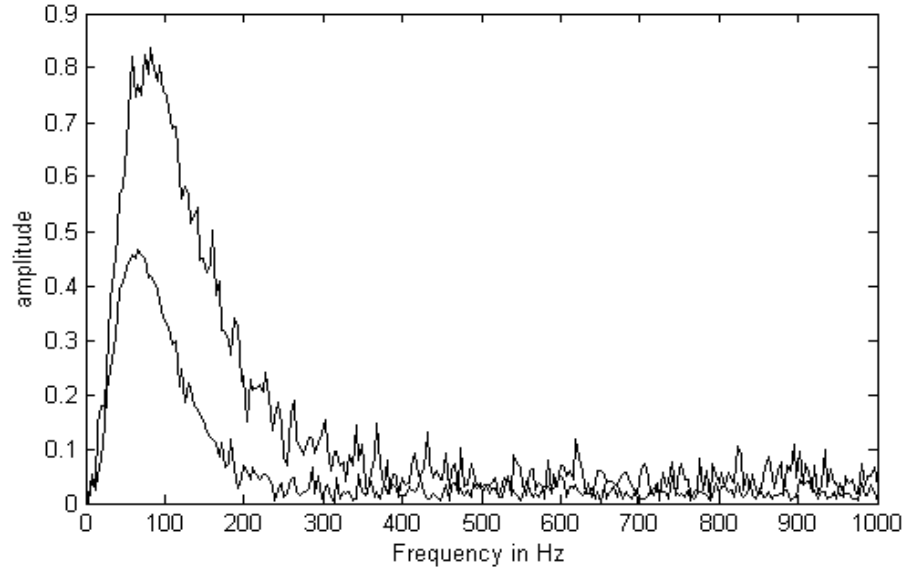
FIG. 10: Amplitude spectra of two traces with signal-to-noise ratio = 5.
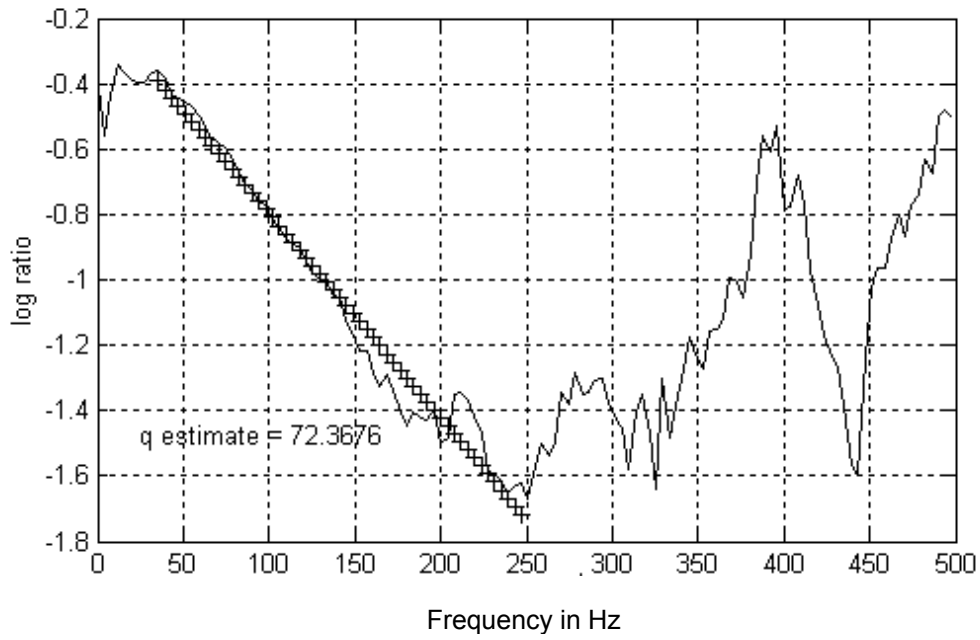
FIG. 11: Q estimate from Figure 10. Given Q value is 50.
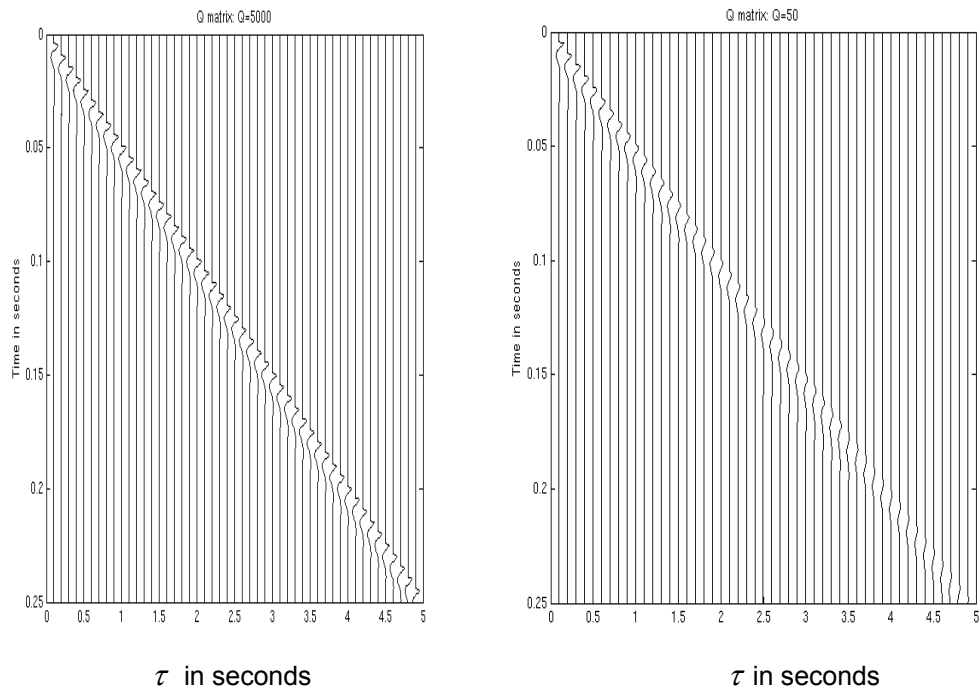
FIG. 12: Impulse responses of Q filters at different times.
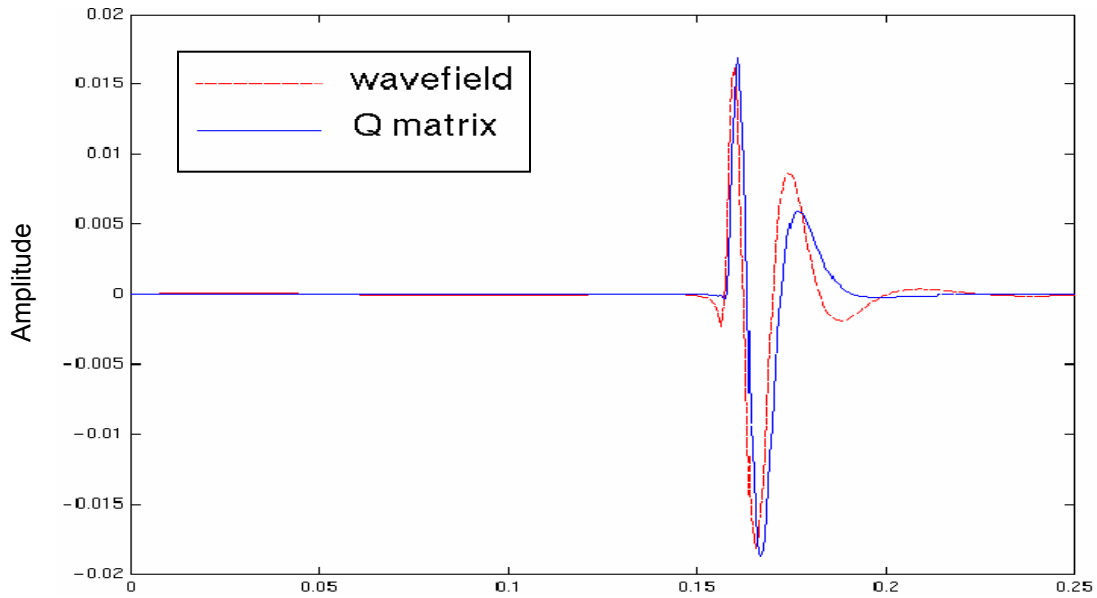
FIG. 13: Comparison of attenuated wavelets from wavefield methods and Q matrix with Q equal to 50.

.
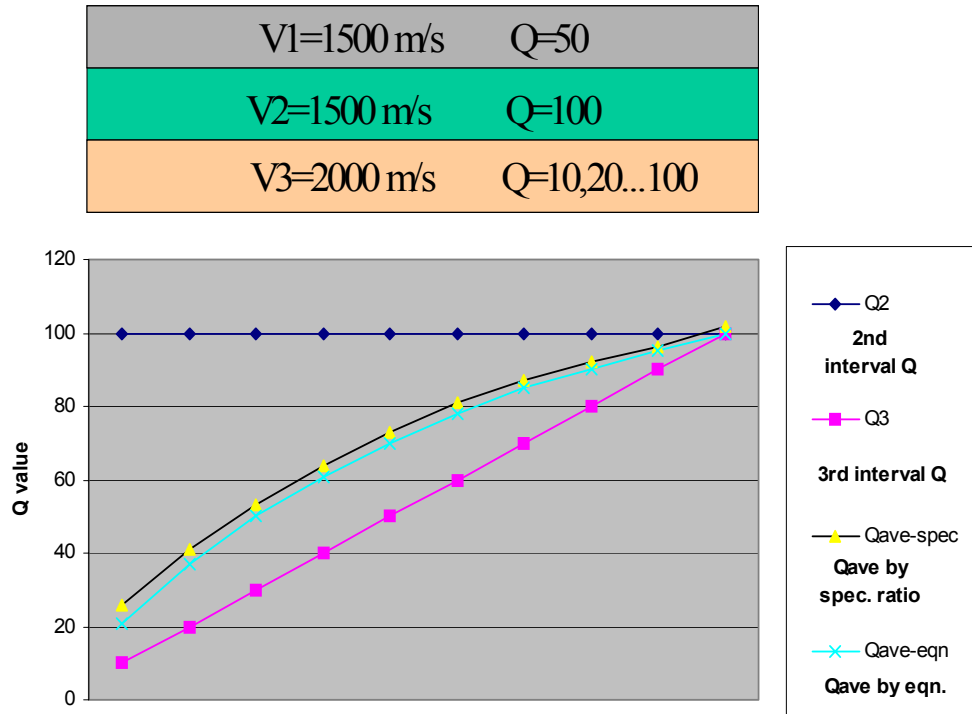
FIG.14: A layered model (Top) with a uniform thickness for each layer and average Q values estimated by spectral ratio methods from the synthetic data and those calculated by the equation (29) from model parameters.